Mechanism of reaction of myoglobin with the lipid hydroperoxide hydroperoxyoctadecadienoic acid

Brandon J. REEDER and Michael T. WILSON[1]

Department of Biological Sciences, Central Campus, University of Essex, Wivenhoe Park, Colchester, Essex CO4 3SQ, U.K.

The reaction between myoglobin and the lipid hydroperoxide 13(*S*)-hydroperoxy-9,11(*cis*,*trans*)-octadecadienoic acid (HPODE) was studied kinetically by spectrophotometric, polarographic and analytical methods. Metmyoglobin catalysed the decomposition of HPODE, resulting in peroxide, oxygen and conjugated diene depletion, together with the transient production of ferryl myoglobin. The reaction stoichiometry was 2:1:1 for peroxide to oxygen to conjugated diene, whereas the myoglobin remained generally intact. This stoichiometry and the rates of change of conjugated diene and ferryl myoglobin concentrations were not completely consistent with previously proposed mechanisms. We propose a novel mechanism in which HPODE reacts with both ferric myoglobin and ferryl myoglobin to form a redox cycle. Both peroxyl and alkoxyl radicals are produced, explaining the observed stoichiometry of peroxide, oxygen and conjugated diene depletion and the transient appearance of ferryl myoglobin. Computer simulation shows that this mechanism is fully capable of reproducing the observed time courses of all components.

INTRODUCTION

The reaction between metmyoglobin (metMb) and H_2O_2 and its contribution to oxidative damage has been extensively researched over many decades. It is well known that ferrylMb resulting from the interaction of H_2O_2 with ferric or ferrous Mb can cause damage to cell membranes, primarily by lipid peroxidation [1–3]. This lipid peroxidation severely damages membrane function; such damage is considered a major pathological role in myocardial reperfusion injuries after ischaemia [4–6]. The ferryl species of Mb has the ability to abstract a hydrogen atom from a lipid (LH) to form an alkyl radical (L$^{\bullet}$). In the presence of oxygen this radical then forms a peroxyl radical (LOO$^{\bullet}$), which can in turn abstract a hydrogen atom from another lipid. The result of the formation of these radicals is the production of lipid hydroperoxides (LOOH) and a cycle of free-radical damage [7–9]. The enzymic formation of unsaturated lipid hydroperoxides, although hazardous, is nevertheless very important in biological systems as it is involved in the intermediate steps in the formation of numerous physiological effectors [10]. Lipid hydroperoxides are normally generated from the oxidation of lipids, that have been liberated from cell membranes by phospholipases, by lipoxygenase enzymes prevalent in most animal and plant cells [11–13]. Lipid hydroperoxides are the precursors of many enzymically and non-enzymically derived potent physiological effectors including leukotrienes, lipoxins, dihydro-eicosanoids and keto-eicosanoids [14–16]. 13(*S*)-Hydroperoxy-9,11(*cis*,*trans*)-octadecadienoic acid (HPODE), used in the investigations reported here, is generated *in vivo* from linoleic acid by plant or animal 15-lipoxygenases [17]:

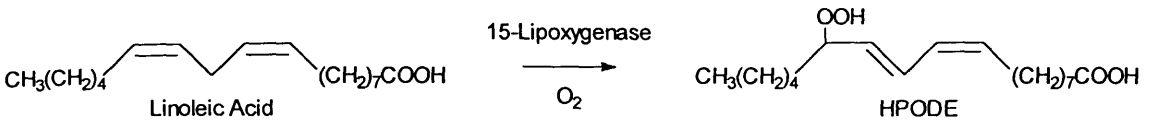

(1)

As well as acting as peroxidants, haem proteins can also act as pseudo-peroxidases, breaking down lipid hydroperoxides formed either by lipoxygenases or by the ferrylMb mechanism described above. Despite a widely accepted mechanism describing lipid peroxidation by haem proteins, the mechanism of degradation of lipid hydroperoxides by haem proteins is less well defined. Many mechanisms have been proposed; one of the most detailed of these relies on the conversion, by ferric haemin, of lipid hydroperoxides to alkoxyl radicals, which then go through a series of rearrangements and termination steps [18–20]. This mechanism explains some of the major components seen by gas chromatography–MS (GC–MS) studies, and also the loss of UV signal associated with conjugated diene observed in some unsaturated lipid hydroperoxides such as HPODE. The mechanism can be formulated as follows:

$$Fe^{3+} + LOOH \rightarrow [Fe^{4+} - OH^{-}]^{3+} + LO^{\bullet} \quad (2)$$

$$LO^{\bullet} \rightarrow epoxyL^{\bullet} \quad (3)$$

$$EpoxyL^{\bullet} + [Fe^{4+} - OH^{-}]^{3+} \rightarrow Fe^{3+} + epoxyLOH \quad (4)$$

In the present study we have examined the interaction of HPODE with haem proteins, primarily metMb, by various quantitative techniques. Some of our results conflict with the mechanism described above for the reaction of haemin.

We have therefore proposed a modified mechanism that more accurately describes the time courses of conjugated diene, oxygen, peroxide and ferryl species in the reaction between HPODE and metMb. The agreement between the computer simulation and the experimental data provides strong support for the proposed

Abbreviations used: Mb, myoglobin; HbA, human haemoglobin A; HPODE, 13(*S*)-hydroperoxy-9,11(*cis,trans*)-octadecadienoic acid; HODE, 13(*S*)-hydroxy-9,11(*cis,trans*)-octadecadienoic acid; triHODE, 9,12,13-trihydroxy-10(*trans*)-octadecaenoic acid; OODE, 13-oxo-9,11(*cis,trans*)-octadecadienoic acid; DTPA, diethylenetriaminepenta-acetic acid; FOX, ferrous oxidation by Xylenol Orange; GC, gas chromatography.

[1] To whom correspondence should be addressed.

mechanism, the basis of which is a redox cycle in which lipid hydroperoxide is consumed in both the formation and decay of the ferryl species, these two reactions resulting in differing lipid products.

EXPERIMENTAL

Materials

Horse heart myoglobin, linoleic acid, soybean lipoxygenase 1 and Xylenol Orange were obtained from Sigma–Aldrich Company Ltd. (Poole, Dorset, U.K.). HPODE and 13-(*S*)-hydroxy-9,11(*cis*,*trans*)-octadecadienoic acid (HODE) HPLC internal standards were obtained from Cascade Biochemicals Ltd (Reading, Berks., U.K.). Ferric sulphate was obtained from BDH Chemical Co. (Lutterworth, Leics., U.K.)

Purification of soybean lipoxygenase 1

Soybean lipoxygenase 1 was further purified from a freeze-dried Sigma–Aldrich preparation by an adaptation of a method developed by Finazzi-Agro et al. [21]. Soybean lipoxygenase 1 (200 mg) was suspended in 25 ml of 0.05 M sodium acetate buffer, pH 5.5, containing 0.05 M NaCl. The suspension was dialysed against the same buffer for 24 h at 4 °C. The dialysed enzyme was then applied to a CM Sephadex C-50 column (200 mm × 15 mm) and washed with 50 ml of 0.05 M sodium acetate buffer, pH 5.5, containing 0.05 M NaCl. The enzyme was eluted with a 0.05–0.3 M linear gradient of NaCl in the sodium acetate buffer, flow rate 0.5 ml/min, and collected in 3 ml fractions. The purity and activity of the enzyme fractions were checked by the UV absorbance of the enzyme (ϵ_{280} 1.4×10^5 $M^{-1} \cdot cm^{-1}$ [22]) and by the activity of linoleic peroxidation as observed by the formation of conjugated diene (ϵ_{234} 2.5×10^4 $M^{-1} \cdot cm^{-1}$ [17]). Active enzyme fractions were pooled and precipitated with 50 %-satd. $(NH_4)_2SO_4$ for storage at 4 °C.

Preparation of HPODE

HPODE was prepared by incubating linoleic acid (2 mM) with purified soybean lipoxygenase 1 (10 μg) in 100 ml of oxygenated 0.1 M sodium borate buffer, pH 9.5, containing 1 % (v/v) ethanol and 10 μM diethylenetriamine penta-acetic acid (DTPA) for 2 h. The enzyme/HPODE solution was acidified to pH 3 and the HPODE was extracted by vigorous shaking with two 100 ml volumes of diethyl ether. The diethyl ether was washed four times with 100 ml of deionized water and the ether was dried with anhydrous $MgSO_4$ (10:1, w/v). The $MgSO_4$ was subsequently removed by filtration. The diethyl ether was removed from the HPODE under a stream of nitrogen. The HPODE was loaded on a silica CC4 column (100 mm × 10 mm) and washed with 50 ml of diethyl ether/cyclohexane (1:9, v/v) and then eluted with 20 % (v/v) diethyl ether. HPODE fractions were detected by the absorbance at 234 nm [17]. The purity of HPODE was determined by HPLC with a straight-phase CN-100 column (244 mm × 4 mm). The 9 isomer of HPODE and hydroxy contaminants were found to be less than 2 % of the overall preparation. HPODE was stored in ethanol at −20 °C.

Preparation of haem proteins

Horse heart Mb was dissolved in the appropriate buffer and centrifuged at 2500 ***g*** for 5 min to remove undissolved material. The metMb supernatant was purified on a Sephadex G-25 column (100 mm × 15 mm). The concentration of metMb was determined spectroscopically by reducing an aliquot of Mb with solid sodium dithionite to form deoxyMb (ϵ_{435} 1.21×10^5 $M^{-1} \cdot cm^{-1}$) [23].

MetMb was reduced to deoxyMb by using excess sodium dithionite. The Mb was reoxygenated and separated from dithionite on a Sephadex G-25 column. The concentration of oxyMb was determined spectrophotometrically as for metMb.

Human haemoglobin A (HbA) was prepared from blood as described by Antonini and Brunori [23]. MetHbA was prepared by incubating oxyHbA with a slight molar excess of potassium ferricyanide. The resulting metHbA was separated from potassium ferricyanide with a Sephadex G-25 column. The concentration of metHbA was determined as for metMb by ϵ_{430} 1.33×10^5 $M^{-1} \cdot cm^{-1}$ (deoxyHbA [22]).

All metMb, metHb and oxyMb samples were used on the day of preparation.

Analytical methods

Spectroscopic measurements were performed with a Varian Cary5E spectrophotometer. Oxygen concentration measurements were made within a quartz cell, housed within a spectrophotometer, by using a Clark oxygen electrode linked to a Clandon oxygen monitor and recorder. Samples were stirred at all times with a micro-stirring rod and a Rank Brothers electronic stirrer located beneath the observation cell.

Straight-phase HPLC was performed on either a Beckman System Gold HPLC fitted with a Walters Wisp auto-sampler and a UV detector and recorder, or a Hewlett Packard 1100 HPLC fitted with a diode array. A LiChrospher straight-phase CN100 column (5 μm particle diameter, 244 mm × 4 mm; Merck, Darmstadt, Germany) was used on both HPLC systems. The flow rate was 1 ml/min of a running solvent consisting of HPLC grade hexane, isopropanol and acetic acid (1000:25:1, by vol.). Under these conditions HPODE eluted approx. 16 min after injection.

Reaction of HPODE with Mb/HbA

All incubations were performed at 25 °C in 0.1 M sodium phosphate buffer containing 10 μM DTPA and 1 % (v/v) ethanol. The Mb concentration was 10 μM unless otherwise stated; the HbA concentration was 2 μM. Samples for HPLC analysis (3 ml volume) were extracted by vigorous shaking with 3 ml of diethyl ether. The ether extracts were dried under a stream of nitrogen and dissolved in 250 μl of HPLC running solvent. Volumes of injected samples were 50 μl.

Ferrous oxidation by Xylenol Orange (FOX) assay

The FOX assay is an indirect method for determining the concentration of peroxy groups, as developed by Wolff [24]. A solution of 300 μM ferric sulphate/120 μM Xylenol Orange was prepared in 0.25 M H_2SO_4. This solution was added to 9 vol. of methanol containing 4 mM butylated hydroxytoluene. The solution was kept at room temperature in the dark and used the day of preparation. MetMb reactions were stopped at the appropriate time by addition of a solution of KCN to a final concentration of 100 μM. The FOX solution (800 μl) was incubated with the sample (200 μl) for 30 min in the dark at room temperature, after which the absorbance was measured at 560 nm. All samples and controls were performed in quadruplicate.

Computer simulations

Kinetic simulations were performed with the PRGEAR and GEAR computer programs distributed by the Further Education Courseware Centre (Lancashire Polytechnic, Preston U.K.).

GEAR is a program for the integration of multistep rate equations with the Gear integration method, as developed by C. W. Gear and adapted to the computer by Stabler and Chesick [25].

RESULTS AND DISCUSSION

The stoichiometry of the reaction between metMb and HPODE

The spectral changes that result from incubating metMb with HPODE are shown in Figure 1. HPODE has a UV spectrum centred on 234 nm, with no contributions above 270 nm. The addition of HPODE to metMb resulted in the partial loss of the 234 nm signal associated with the conjugated diene structure of HPODE (Figure 1B). The rate of decay at 234 nm increased as the concentration of metMb was increased. From this we conclude that Mb acts as a catalyst for the reaction. The signal at 234 nm decayed to $35 \pm 3\,\%$ (S.D.) of its original absorbance intensity irrespective of the concentration of HPODE used. The signal remaining at 234 nm was not due to unreacted HPODE as it was not lost on further addition of metMb (see also HPLC below). The 234 nm signal decay followed a pseudo-first-order time course with a rate constant of $4.5 \times 10^{-3}\ s^{-1}$ and the reaction was essentially complete within 10 min (Figure 2). Accompanying the HPODE UV signal decay was a loss of absorbance at 408 nm associated with the Soret peak of metMb, and the appearance of a shoulder at 425 nm (Figure 1). This is consistent with a bathochromic (red) shift of the Soret band of a fraction of the Mb. Once degradation of HPODE was complete, a gradual return of the Soret spectrum towards the initial metMb spectrum was observed (Figure 3); however, this 'relaxation' was only partial and did not fully return to the original metMb spectrum. The addition of excess sodium dithionite after completion of the reaction (30 min) resulted in approx. 90 % of the expected deoxy (ferrous) Mb absorbance at 435 nm, showing that 10 % of the haem moiety had degraded under the conditions described (results not shown). The EPR spectrum of this reaction mixture revealed a small production (approx. 10 %) of rhombic $g = 4.35$ signal associated with non-haem iron from degraded Mb, confirming that most of the myoglobin remained intact during the course of the reaction. The time course of the 234 nm signal is shown in Figure 2, where it is compared with oxygen consumption during the reaction. The rate constant for oxygen consumption was $4.7 \times 10^{-3}\ s^{-1}$, which is identical, within our experimental error, to that of the decay of the conjugated diene. We conclude that oxygen consumption is linked to conjugated diene decay through a common mechanistic step.

Figure 2 compares the concentration of the peroxy group with the estimated conjugated diene concentration throughout the reaction. The HPLC data agreed well with the data from the FOX assay, both HPLC and FOX assays detecting the HPODE peroxy group. Figure 2 shows that peroxide depletion also has essentially the same rate constant as the oxygen consumption and conjugated diene depletion (see above). However, the magnitude of peroxide decay is almost twice that observed for the oxygen consumption; thus for every two HPODE molecules used, one molecule of oxygen is consumed. A very similar stoichiometry is seen between peroxide and conjugated diene. Figure 2 gives an apparent stoichiometry of 2 peroxides consumed to 1.2 conjugated dienes lost. However, this calculation is based on the conjugated dienes having the same absorption coefficient as HPODE. The HPLC analysis (below) shows that in fact the conjugated diene possesses a lower absorption coefficient owing to the presence of oxodienes, giving an overall stoichiometry of 2:1:1 for oxygen consumption to conjugated diene depletion to peroxide consumption.

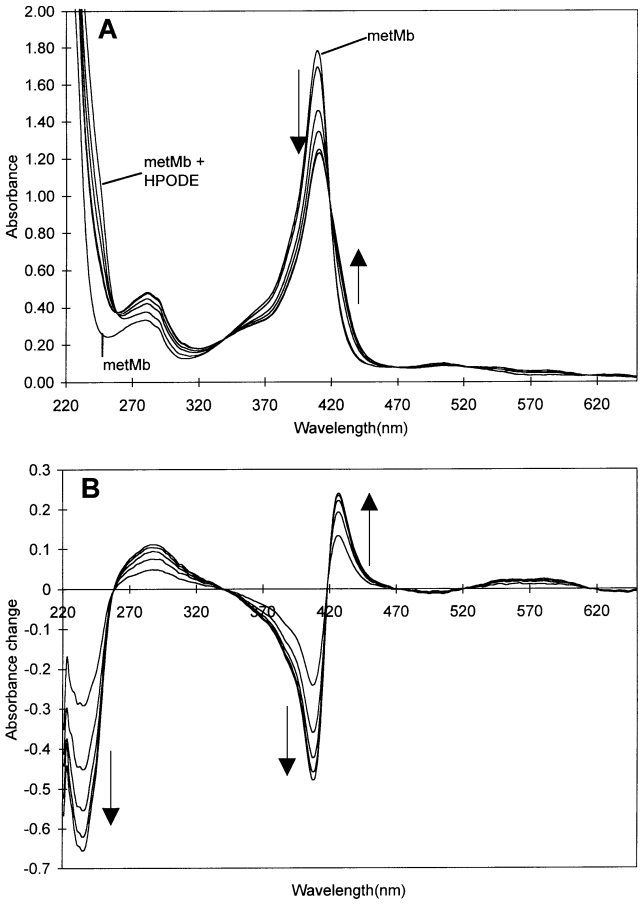

Figure 1 Reaction of HPODE with metMb followed optically

(**A**) Spectra were taken before and immediately after the addition of HPODE (50 μM) to metMb (10 μM). Additional spectra were taken at 2 min intervals for 12 min. (**B**) The spectral contribution of metMb was subtracted to give difference spectra for the reaction. Reactions were performed in 0.1 M sodium phosphate buffer, pH 7.4, containing 10 μM DTPA and 1 % (v/v) ethanol. Temperatures were kept at 25 °C throughout.

Detection and quantification of ferryl myoglobin by sulphide addition

It has previously been shown that the addition of ethyl hydrogen peroxide to metMb produces ferrylMb [26,27], and the addition of Na_2S to this ferryl species produces a characteristic peak at approx. 617 nm owing to the addition of sulphur to the haem porphyrin ring, resulting in ferrous sulphMb [28]. The addition of Na_2S (1 mM) to an incubated sample of metMb and HPODE showed a similar peak at 617 nm, indicating the formation of sulphMb from ferrylMb (Figure 3). Also present in the spectrum were two peaks at 555 and 595 nm, which were produced from an adduct of sulphide with metMb, confirming the presence of both ferrylMb and metMb in the reaction mixture. Using the absorption coefficient of sulphMb ($\Delta\epsilon_{617-600}$ 10.5 $mM^{-1} \cdot cm^{-1}$ [29]) we calculated that approx. 40 % of the myoglobin existed in the ferryl form at the time of sulphide addition (15 min into incubation). The addition of Na_2S (1 mM) at specific incubation times enabled the production and decay of ferrylMb to be monitored. The profile of ferrylMb production compared with the Soret spectral changes is shown in Figure 4. The optical changes at 408 and 425 nm parallel the ferrylMb production. The decay of the Soret 425 nm band and the restoration of the

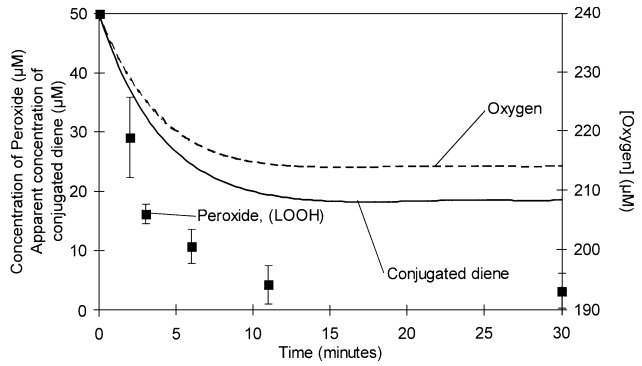

Figure 2 Time course for the reaction of HPODE with metMb

Time course of conjugated diene and lipid peroxide depletion compared with oxygen consumption by the HPODE/metMb reaction. The depletion of HPODE conjugated diene (solid line, left ordinate) was measured spectrally at 234 nm and converted to concentration by using the HPODE absorption coefficient (see the Experimental section). Oxygen concentration (broken line, right ordinate) was measured by a Clark oxygen electrode simultaneously with the spectral observations. Peroxide measurements (■, left ordinate) were performed separately with an amalgamation of HPLC and FOX assays (see the Experimental section).

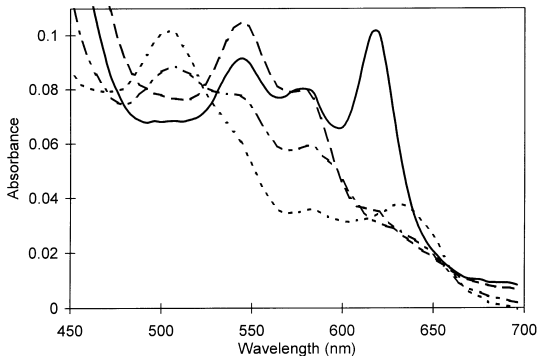

Figure 3 Formation of ferrylMb in the reaction between HPODE and metMb

The spectrum of metMb (dot–dashed line) with absorbance maxima at 505 and 635 nm, is shown before HPODE addition. HPODE was incubated with metMb and the spectrum was taken at 15 min incubation time (dotted line). The addition of Na_2S (1 mM) to either the metMb (broken line) or ferrylMb (solid line) gave characteristic spectra.

408 nm band do not, however, precisely mirror the ferrylMb decay. The Soret spectral changes are caused by an amalgamation of ferrylMb decay and other factors affecting the haem moiety, e.g. haem decay and protein conformational changes.

Comparison with other haem proteins

Human HbA depleted the conjugated diene of HPODE with a rate constant of 2.5×10^{-3} s^{-1} (2 μM haem). Unlike horse heart Mb, HbA showed a marked haem degradation, as observed from a large decrease in signal intensity over the entire Soret region (Figure 5A). This degradation of the haem obscures any signal due to the ferrylMb, which in any case seems small. However, it is possible to observe the formation of a ferrylMb species from the reaction of liposomes with αDBBF HbA [α chains cross-linked with bis-(3,5,-dibromosalicyl)fumarate], which gives similar optical changes to those observed with metMb and HPODE [30]. Ferrous oxyMb also reacts with HPODE, although at a lower rate than that observed with metMb (rate constant of

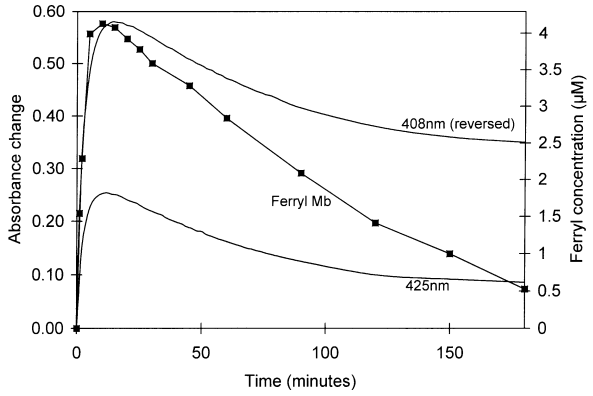

Figure 4 Time course of ferrylMb production and decay

FerrylMb concentrations were measured with the Na_2S assay as described in the Experimental section; see also Figure 3. Optical measurements were taken simultaneously at 408 and 425 nm.

conjugated diene decay for oxyMb, 1.2×10^{-3} s^{-1}). The spectral perturbations of the Soret region of oxyMb are more complex than those seen in the metMb reaction. The difference spectra (Figure 5B) provide evidence that more than one transition occurs.

HPLC analysis of the lipid products of the reaction of MetMb with HPODE

The lipid products extracted after the incubation of HPODE with metMb were analysed on a straight-phase CN100 HPLC column; the results are presented in Figure 6(A). Controls, in the absence of metMb, showed that only HPODE was present, being eluted at 16.5 min and giving a single peak (Figure 6A, trace I). The spectrum of this peak is shown in Figure 6(B), trace I. The elution profile, monitored at 234 nm, after a 30 min incubation of metMb with HPODE, is shown in Figure 6(A), trace II; a major product can be observed being eluted after 10 min. The spectrum of this compound is similar to that of HPODE, having a maximum absorbance at 234 nm (Figure 6B, trace II). Another major product was eluted at 9.6 min; this product absorbed poorly at 234 nm but had a peak maximum at approx. 280 nm (Figure 6A, trace III, and Figure 6B, trace III). Peaks that were eluted in less than 5 min were of protein fragments extracted with the lipid products. Several other minor products were observed, each having spectral properties similar to either the 9.6 or 10 min eluates. From further HPLC studies with $^{14}C_1$-labelled HPODE as a substrate, several other components were detected that had no corresponding UV contribution owing to the lack of conjugated diene structure (results not shown). This is consistent with GC–MS results previously reported for the reaction between HPODE and haemin, which yields five major products: HODE, 13-oxo-9,11(*cis*,*trans*)-octadecadienoic acid (OODE), two epoxy alcohols and 9,12,13-trihydroxy-10(*trans*)-octadecaenoic acid (triHODE) [18], the last three having no conjugated diene structure. The 13-isomer of HODE has the same UV spectrum and absorption coefficient as HPODE [17], whereas OODE has a UV spectrum shifted to a longer wavelength by the 9,11-*cis*,*trans*-conjugated diene's itself being conjugated to a carbonyl group on the 13th carbon atom. This explains the somewhat greater loss of absorbance at the wavelength of 234 nm

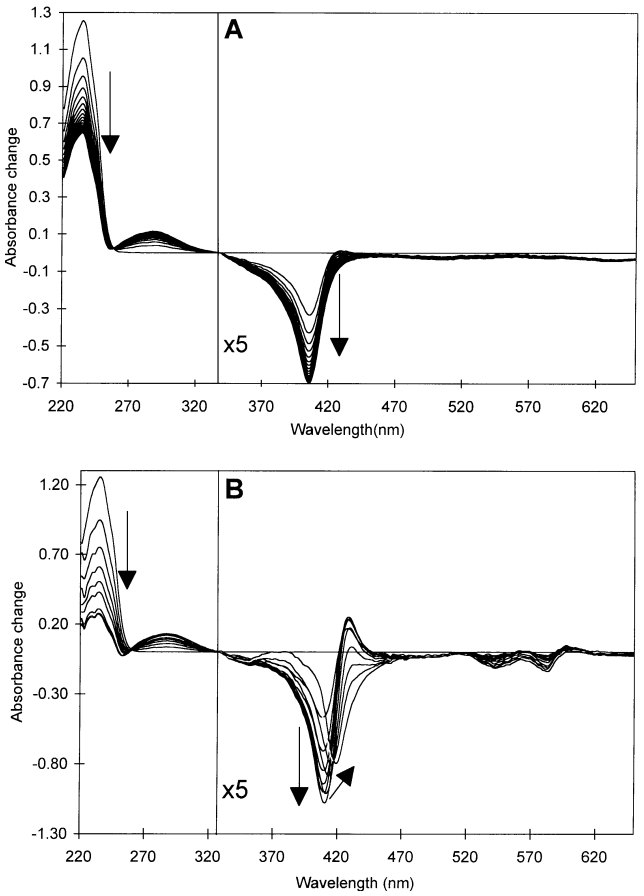

Figure 5 Interactions of HPODE with metHbA or oxyMb monitored optically

HPODE (50 μM) was added to metHbA (2 μM; **A**) or oxy(ferrous)Mb (10 μM; **B**). Subsequent spectra were taken at 2 min intervals for the metHbA reaction and 5 min intervals for the first 30 min, then every 30 min for the oxyMb reaction. In both cases extensive degradation of the conjugated diene signal of the lipid can be observed (234 nm). HbA also shows extensive degradation (approx. 45%) with no evidence of the ferryl Soret shoulder. The Soret spectral changes for the oxyMb reaction are complex, with ferrous, ferric and ferryl species present.

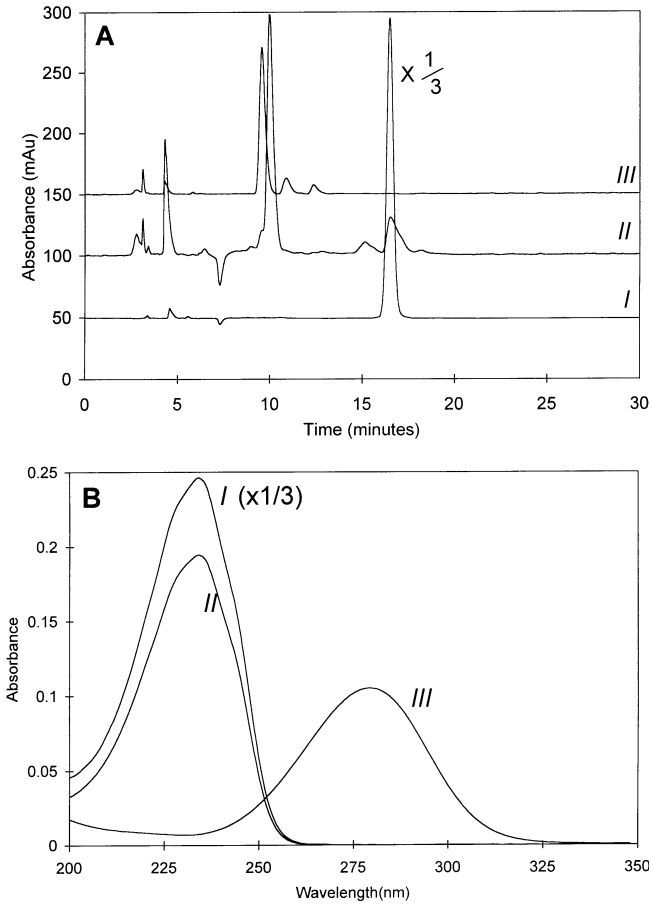

Figure 6 HPLC analysis of the products of the reaction between HPODE and metMb

Lipid products were detected by UV HPLC before (controls) and after incubation with metMb. Incubation conditions were as described in the legend to Figure 1. (**A**) Trace I, Straight-phase HPLC chromatography of an HPODE standard, detected at 234 nm compared with post-incubation products detected at 234 nm (trace II) and 280 nm (trace III). Both wavelengths were monitored simultaneously; chromatograms are offset by 50 m-absorbance units for clarity of presentation. (**B**) Diode array spectra of the major elution peaks from (**A**). HPODE was eluted at 16.5 min (trace I), HODE at 10.0 min (trace II) and OODE at 9.6 min (trace III). After 30 min of incubation in the presence or absence of metMb, the lipid products were extracted with diethyl ether as described in the Experimental section. The 9- and 13-isomers of HPODE and the 9-and 13-isomers of HODE were used for calibration purposes.

than was initially expected. Thus HODE and OODE are likely candidates for the 10.0 and 9.6 min post-reaction eluate components respectively.

Mechanism of the reaction of myoglobin with HPODE

The cycle through which the haem passes involves the production of ferryl haem iron (see Figures 1 and 6), in agreement with the conclusions of Kanner and Harel [7] and Dix and Marnett [18]. The addition of radical scavengers such as butylated hydroxytoluene did not inhibit peroxide consumption, indicating that the reaction is not mediated by radicals that escape the haem pocket. This lack of involvement of radicals is supported by the absence of a lag phase in the time courses of oxygen uptake and the change in the conjugated diene and peroxide concentrations. Lag phases are characteristic of radical-mediated reactions [31]. As outlined in the Introduction section, a mechanism has previously been proposed to account for the depletion of conjugated diene in the reaction between haemin and HPODE, suggesting a catalytic ferric/ferryl redox cycle. This mechanism is, however, not fully consistent with the experimental results that we report here for the reaction between HPODE and haem proteins. We therefore propose a mechanism that, although containing elements in common with this earlier proposal, e.g. a ferric/ferryl cycle, differs from this by suggesting that the cycle is driven in both directions by peroxide (Scheme 1) as opposed to peroxide and a lipid-based radical (see eqns. 2–4).

The central feature of the mechanism described in Scheme 1 is the reaction between ferricMb and the peroxide group of HPODE (LOOH), generating ferrylMb and an alkoxyl radical (LO$^{\bullet}$). This ferryl species reacts with a further molecule of HPODE returning the protein to the ferric form and generating a peroxyl radical (LOO$^{\bullet}$). We propose, in keeping with the extensive literature, that the alkoxyl radical rearranges to form an epoxide bearing a carbon-centred radical (epoxyL$^{\bullet}$), losing the conjugated diene structure. This epoxyL$^{\bullet}$ radical reacts with molecular oxygen to form an epoxy peroxide radical [32–34]:

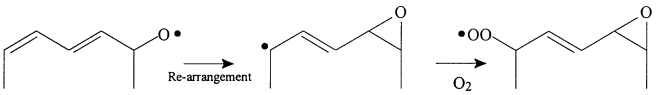

The reactions discussed so far account for the loss of two molecules of peroxide and the consumption of one molecule of oxygen, in agreement with the observed stoichiometry (Figure 2). The mechanism also predicts the loss of one conjugated diene per redox cycle.

The termination of peroxyl radicals via the concerted process results in the production of lipid ketones and alcohols [35]. This is consistent with the HPLC data and previous GC–MS studies showing two of the major products to be HODE and OODE. The production of singlet oxygen, also predicted by the concerted process of peroxyl termination, might be expected to yield molecular oxygen, but this was not observed polarographically. A similar situation has been noted for the reaction between cumene hydroperoxide or t-butyl hydroperoxide and haemin [36]. The exact nature of peroxyl radical termination is complex and requires further investigation.

Comparison with other mechanisms and computer simulations of reaction mechanism

We believe that our mechanism is novel and is better able to account for the experimental results than the previously accepted mechanism (eqns. 2–4). This latter mechanism does not predict the observed stoichiometry for oxygen consumption (i.e. 1 oxygen to 2 peroxides) and indeed suggests a non-integral and variable stoichiometry depending on the fate of the epoxyalkyl radical, which might diffuse from the haem pocket, reacting with oxygen, and become reduced to form an epoxide alcohol. Furthermore, whereas the mechanism in Scheme 1 and Figure 7 show a peroxide to conjugated diene stoichiometry of 2:1, the earlier mechanism gives this ratio as 1:1, as each hydroperoxide yields an epoxide alcohol.

Our proposed mechanism also explains the appearance of four (HODE, OODE and two epoxide alcohol isomers) of the five major products observed in previous GC–MS studies [18–20]. The previously accepted mechanism can account for only two of the five major products, namely both epoxide alcohol isomers. The detection of the fifth major product, triHODE, by GC–MS is not predicted by either mechanism. It can be noted, however, that preliminary MS measurements with the more direct and gentle technique of negative electrospray ionization MS on metMb and HPODE show no evidence of triHODE as a major product (B. J. Reeder, M. T. Wilson, D. J. Hayes and P. Francis, unpublished work). Whether the differences between haem proteins and haemin are due to the different mechanistic features for the two haem compounds or are due to the hydration of epoxides (from extensive sample handling required to prepare lipids for GC–MS) remains to be decided.

Thus the mechanism in Scheme 1 predicts both the observed stoichiometry of the reaction and the pattern of formation of products. It remains to be shown that it can reproduce the time courses found experimentally and reported in Figures 1, 2 and 4. We have therefore used computer simulations to test whether the Scheme can reproduce these kinetics. Figure 7 shows the correspondence between the experimental data and the time courses simulated on the basis of the mechanism in Scheme 1. The simulation for oxygen and peroxide concentrations are close to the experimental results. We also found a good correspondence with the UV time course, on the assumption that OODE has a lower absorption coefficient at 234 nm. The simulation, however, showed that the initial rate for ferrylMb production was higher than that found experimentally. This simulation was brought into coincidence with the experimental results by the addition of an initial 'slow step' for metMb conversion to ferrylMb for approx. 50 % of the metMb population. This requirement might reflect the existence of an exogenous ligand, such as water or hydroxide, blocking the sixth co-ordination site of the haem. Alternatively it might result from a protein conformational modification caused by free-radical damage, allowing greater access to the haem pocket. This conjecture can be substantiated by the effect of further additions of HPODE to the post-reaction mixture, which showed an increase in the initial rate of conjugated diene consumption from 41 to 78 nM/s (B. J. Reeder and M. T.

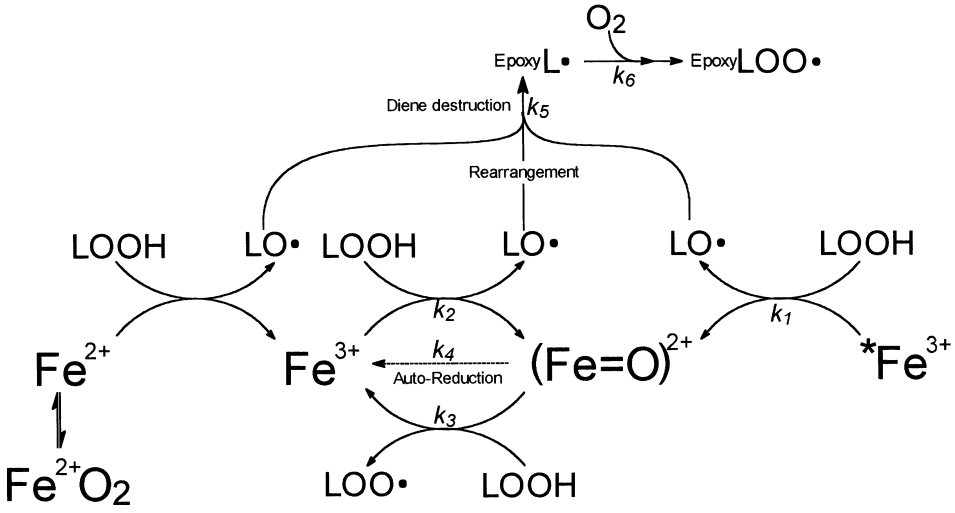

Scheme 1 Reaction of Mb with the lipid hydroperoxide, HPODE

Ferrous or ferric(met)Mb is oxidized by HPODE (LOOH) to form alkoxyl radicals (LO•), which spontaneously rearrange to form epoxyalkyl radicals (epoxyL•) and in so doing destroy the conjugated diene. In the presence of oxygen the epoxyalkyl radicals form epoxyperoxyl radicals (epoxyLOO•). HPODE reduces ferrylMb to metMb, forming a peroxyl radical (LOO•) with intact conjugated diene structure. Two forms of metMb are illustrated, a slow ($*Fe^{3+}$) and fast (Fe^{3+}) reacting population; these two forms are required to simulate the transient ferrylMb production and their existence is also suggested from serial HPODE addition (see the text). Rates k_1 to k_6 are used in the GEAR simulations (see the text).

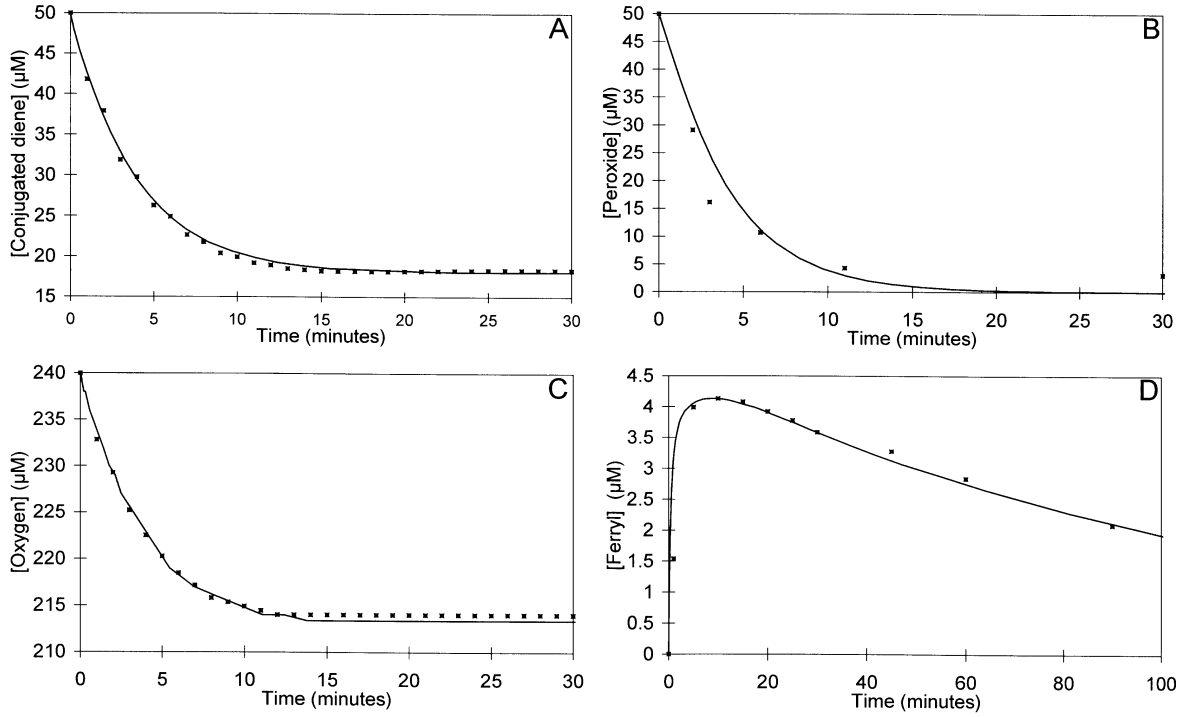

Figure 7 Simulations of conjugated diene depletion (A), peroxide depletion (B), oxygen consumption (C) and ferryl production and decay (D) with the mechanism proposed in Scheme 1 for the reaction between HPODE (50 μM) and metMb (10 μM)

Simulations (solid lines) are overlaid with the respective data (■) from Figures 1, 2 and 4. Simulations were performed on the GEAR program by input of the following processes and rate constants. For the production of ferrylMb and LO$^{\bullet}$ from metMb and LOOH the rate constants (k_1, k_2) were 1.7×10^2 and 4.3×10^2 $M^{-1} \cdot s^{-1}$ for slow and fast populations respectively (see text). For the production of metMb and LOO$^{\bullet}$ from ferrylMb and LOOH the rate constant (k_3) was 5.3×10^2 $M^{-1} \cdot s^{-1}$, that for metMb produced from ferrylMb auto-reduction (k_4) was 1.5×10^{-4} $M^{-1} \cdot s^{-1}$. LO$^{\bullet}$ rearrangement and oxygen addition were set to 10^8 s^{-1} and 10^8 M^{-1} s^{-1} (k_5, k_6) respectively. Initial concentrations were: $^{*}Fe^{3+}$, 5 μM; Fe^{3+}, 5 μM; LOOH, 50 μM; O_2, 240 μM; all other components were set to zero. The simulation was sensitive to the values of k_1 to k_4 such that a 5% change in any of these values resulted in a significantly worse reproduction of the time courses. Values of k_5 and k_6 were set high to ensure that they were not rate-limiting. All metMb/HPODE incubation conditions were as described in the legend to Figure 1.

Wilson, unpublished work). Such a phenomenon of rate enhancement was not observed in the haemin/HPODE reaction.

B.J.R. thanks the BBSRC and Glaxo-Wellcome for financial support (CASE studentship), and David J. Hayes (Glaxo-Wellcome) and David Stone for their technical assistance.

REFERENCES

1 Newman, E. S. R., Rice-Evans, C. A. and Davies, M. J. (1991) Biochem. Biophys. Res. Commun. **179**, 1414–1419
2 Sarti, P., Hogg, N., Darley-Usmar, V. M., Sanna, M. T. and Wilson, M. T. (1994) Biochim. Biophys. Acta **1208**, 38–44
3 Hogg, N., Rice-Evans, C., Darley-Usmar, V. M., Wilson, M. T., Paganga, G. and Bourne, L. (1994) Arch. Biochem. Biophys. **313**, 39–44
4 Kelman, D. J., DeGray, J. A. and Mason, R. P. (1994) J. Biol. Chem. **269**, 7458–7463
5 Sakamoto, A., Ohnishi, S. T., Ohnishi, T. and Ogawa, R. (1991) Brain Res. **554**, 186–192
6 Sakamoto, A., Ohnishi, S. T., Ohnishi, T. and Ogawa, R. (1991) Free Radical Biol. Med. **11**, 385–391
7 Kanner, J. and Harel, S. (1985) Arch. Biochem. Biophys. **237**, 314–321
8 Davies, M. J. (1988) Biochim. Biophys. Acta **964**, 28–35
9 Rao, S. I., Wilks, A., Hamberg, M. and Ortiz de Montellano, P. R. (1994) J. Biol. Chem. **269**, 7210–7216
10 Chamitrat, W. and Mason, R. P. (1989) J. Biol. Chem. **264**, 20968–20973
11 Sehan, C. N. (1994) Biochim. Biophys. Acta **1212**, 1–25
12 Kühn, H., Schewe, T. and Rapoport, S. M. (1986) Adv. Enzymol. **58**, 273–311
13 Ford-Hutchinson, A. W. (1991) Eicosanoids **4**, 65–74
14 Schewe, T., Rapoport, S. M. and Kühn, H. (1986) Adv. Enzymol. **58**, 191–272
15 Gardner, H. W. (1991) Biochim. Biophys. Acta **1084**, 221–239
16 Siedow, J. N. (1991) Annu. Rev. Plant Physiol. Plant Mol. Biol. **42**, 145–188
17 Egmond, M. R., Brunori, M. and Fasella, P. M. (1976) Eur. J. Biochem. **61**, 93–100
18 Dix, T. A. and Marnett, L. J. (1985) J. Biol. Chem. **260**, 5351–5357
19 Dix, T. A., Fontana, R., Panthani, A. and Marnett, L. J. (1985) J. Biol. Chem. **260**, 5358–5365
20 Hamberg, M. (1983) Biochim. Biophys. Acta **752**, 191–197
21 Finazzi-Agro, A., Avigliano, L., Veldink, G. A., Vliegenthart, J. F. G. and Boldingh, J. (1973) Biochim. Biophys. Acta **326**, 462–470
22 Axelrod, B., Cheesebrough, T. M. and Lafksos, S. (1981) Methods Enzymol. **71**, 441–451
23 Antonini, E. and Brunori, M. (1971) in Frontiers in Biology, vol. 21 (Neuberger, A. and Tatum, E. L., eds.), pp. 13–52, North-Holland, Amsterdam
24 Wolff, S. P. (1994) Methods Enzymol. **233**, 182–189
25 Stabler, R. N. and Chesick, J. P. (1978) Int. J. Chem. Kinet. **10**, 461–469
26 Tamura, M., Oshino, N., Chance, B. and Silver, I. A. (1978) Arch. Biochem. Biophys. **191**, 8–22
27 Mairino, M., Ursini, F. and Cadenas, E. (1994) Free Radical Biol. Med. **16**, 661–667
28 Walters, F. P., Kennedy, F. G. and Jones, D. P. (1983) FEBS Lett. **163**, 292–296
29 Berzofsky, J. A., Peisach, J. and Blumberg, W. E. (1971) J. Biol. Chem. **246**, 3367–3377
30 Rogers, M. S., Patel, R. P., Reeder, B. J., Sarti, P., Wilson, M. T. and Alayash, A. I. (1995) Biochem. J. **310**, 827–833
31 Sarti, P., Hogg, N., Darley Usmar, V. M., Sanna, M. T. and Wilson, M. T. (1994) Biochim. Biophys. Acta **1208**, 38–44
32 Wilcox, A. L. and Marnett, L. J. (1993) Chem. Res. Toxicol. **6**, 413–416
33 Aoshima, H., Yoshida, Y. and Taniguchi, H. (1986) Agric. Biol. Chem. **50**, 1777–1783
34 Pace-Asciak, C. R. (1984) Biochim. Biophys. Acta **793**, 485–488
35 Niu, Q. J. and Mendenhall, G. D. (1992) J. Am. Chem. Soc. **114**, 165–172
36 Kalyanaraman, B., Mottley, C. and Mason, R. P. (1983) J. Biol. Chem. **258**, 3855–3858

Received 20 August 1997/7 November 1997; accepted 21 November 1997